Dispersion of Heavy Particles by Turbulent Motion

LIAN-PING WANG* AND DAVID E. STOCK

Department of Mechanical and Materials Engineering, Washington State University, Pullman, Washington

(Manuscript received 28 April 1992, in final form 9 September 1992)

ABSTRACT

Accurate prediction of heavy particle dispersion in turbulent flows requires a simultaneous consideration of particle's inertia and particle's drift velocity. A mathematically simple and physically comprehensive analysis was developed to solve the dispersion statistics of heavy particles in a homogeneous and isotropic turbulent flow. Normalized particle diffusivity, rms fluctuating velocity, and Lagrangian integral time were related by algebraic equations to three dimensionless parameters: the inertia parameter, the drift parameter, and the turbulence structure parameter. When the drift parameter is large, dispersion scales are very sensitive to the inertia parameter. Heavy particles were found to disperse faster than fluid elements if the inertia parameter controls the dispersion and slower than fluid elements if the drift parameter governs the dispersion. This finding explains previous "contradictory" dispersion data observed in experimental measurements. Not only the particle time scale but also the particle velocity scale in the direction normal to the drift were shown to be less than their respective values in the direction parallel to the drift due to the effect of fluid continuity. Use of nonlinear drag law in the analysis was made possible by using an effective inertia and an effective drift. Results of the analysis were compared with numerical simulation and other analytical studies.

1. Introduction

Heavy particles are any small particles in the flow with a density much larger than the density of the fluid. Heavy particles have a free fall velocity that is of the order of the fluid rms velocity. Heavy particle dispersion is found in many industrial and natural flows. Examples include the combustion of pulverized coal, the pneumatic transport, electrostatic precipitation, and dust transport in the atmospheric boundary layer. The dispersion of aerosols can also be viewed as an extension to the problem of atmospheric diffusion of a passive scalar. We are interested in the dispersion characteristics of the particles when suspended in and driven by a stationary and homogeneous turbulent flow. Although this is a simple flow, many important flows closely resemble this simple flow, and it represents a building block toward understanding dispersion in more complex flows.

The dynamic response of a heavy particle to a turbulent flow is different from that of a fluid element because of the particle's inertia and body forces acting on the particle, typically gravity. The latter gives a heavy particle a finite drift velocity relative to the mean motion of the surrounding fluid (also called the settling velocity or the free-fall velocity). Therefore, heavy particle dispersion is a more complex problem than the diffusion of fluid packets, gases, or small light particles. Nevertheless, most analytical studies of heavy particle dispersion (Tchen 1947; Yudine 1959; Csanady 1963; Meek and Jones 1973; Reeks 1977; Pismen and Nir 1978) use the Lagrangian formulation pioneered by Taylor (1921), which was originally introduced for the turbulent diffusion of fluid elements. The particle dispersion coefficient, $\epsilon_{ij}^p(\tau)$, is naturally related to the velocity correlation of a heavy particle along its trajectory by

$$\epsilon_{ij}^p(\tau) = \int_0^\tau \langle v_i(0)v_j(t)\rangle dt, \qquad (1.1)$$

where $v_j(t)$ is the jth component of the particle velocity relative to its mean at time t and the angle brackets indicate an ensemble average over all realizations of the particle motion. In general, $v_j(t)$ is related to the instantaneous fluid velocity at the particle's location, $u_j^p(t)$, the particle's inertia, and the particle's drift velocity; $u_j^p(t)$ is an unknown nonlinear function of the particle location, which in turn, is related to the particle's velocity. This intrinsic nonlinearity in $u_j^p(t)$ makes it impossible to solve the dynamic equations of motion describing the time evolution of the particle velocity, as first discussed by Lumley (1957). The Lagrangian particle velocity correlation, the integrand of (1.1), is central to the dispersion process but, unfortunately, no general exact solution exists.

* Current affiliation: Department of Mechanical Engineering, The Pennsylvania State University, University Park, Pennsylvania.

Corresponding author address: Dr. David E. Stock, Department of Mechanical and Materials Engineering, Washington State University, Pullman, WA 99164-2920.

Tchen (1947) provided the first approximate solution to the dispersion problem by assuming that a particle was always confined to the same fluid element, namely, that $u^p(t)$ was the same as the fluid velocity along a fluid-element trajectory. Such an assumption requires that both the inertia and drift velocity of the particle are small; thus, the results of Tchen's analysis are of limited use (Hinze 1975). Another consequence of the assumption is that the calculated long-time dispersion coefficient of heavy particles is the same as the long-time diffusion coefficient of fluid elements. Soo (1956) attempted to formulate the dispersion statistics of particles in an isotropic turbulent stream but made no improvement. He also misinterpreted the particle diffusivity by using the correlation microscale to replace the integral scale. Friedlander (1957) considered the case of particles with large inertia and zero drift velocity. He realized that the fluid velocity correlation seen by a heavy particle tended to be the fluid Eulerian velocity correlation in the limit of large inertia. Meek and Jones (1973) extended the past work to include finite inertia and drift velocity; however, they made the same assumption as Tchen, that the correlation time of $u_i^p(t)$ was simply the fluid's Lagrangian integral time. Yudine (1959) and Csanady (1963) studied the other extreme of zero inertia and large drift velocity. For this case the heavy particle follows the fluid velocity fluctuations exactly, so that the particle root-mean-square (rms) fluctuating velocity is the same as the fluid rms fluctuating velocity, u_0. Also, the fluid velocity correlation seen by a heavy particle, $\langle u_i^p(0)u_j^p(\tau)\rangle$, can be approximated by the Eulerian spatial velocity correlation of the flow, $\langle u_i(\mathbf{0}, 0)u_j(\mathbf{v}_d\tau, 0)\rangle$, assuming $u_j(\mathbf{x}, t)$ is the jth component of fluid Eulerian velocity in a frame of reference moving with the mean fluid velocity and $\mathbf{v}_d$ is the drift velocity [see Eq. (2.4) for detailed definition]. The effect of the drift velocity on the velocity correlation is known as the "crossing-trajectories effect," which was first introduced by Yudine (1959). The approximation of zero inertia and large drift velocity is valid only when the drift velocity is so large that the time scale L_f/v_d is small compared with the eddy decay time (Reeks 1977). Here L_f is the integral length scale of the longitudinal spatial velocity correlation of the Eulerian flow field. In addition to the time scale L_f/v_d, Csanady (1963) introduces another time scale L_f/u_0 representing the effect of eddy decay on the velocity correlation. By assuming a form for $\langle u_i^p(0)u_j^p(\tau)\rangle$ consistent with exponential Eulerian spatial and exponential Lagrangian fluid–point correlations, he obtained a relation for the dispersion coefficient in the vertical direction (parallel to the drift velocity) of the form

$$\epsilon_{33}^p(\infty) = \epsilon^f(\infty)\left(1 + \frac{T_L^2 v_d^2}{L_f^2}\right)^{-1/2}, \qquad (1.2)$$

where T_L is the fluid Lagrangian integral time scale and the superscript f refers to the fluid. Since the length scale for the transverse velocity correlation of the Eulerian flow field is half L_f for an isotropic stationary turbulent flow, Csanady suggested a relation for the dispersion coefficient in the horizontal directions as

$$\epsilon_{11}^p(\infty) = \epsilon_{22}^p(\infty) = \epsilon^f(\infty)\left(1 + 4\frac{T_L^2 v_d^2}{L_f^2}\right)^{-1/2}. \qquad (1.3)$$

From (1.2) and (1.3) we see that the effect of increasing v_d is to reduce the particle dispersion coefficient both in the direction parallel as well as normal to $\mathbf{v}_d$. This reduction is totally due to the reduction in the particle velocity correlation times caused by the effect of crossing trajectories. In the limit as $v_d/u_0 \to \infty$, the dispersion coefficient normal to $\mathbf{v}_d$ is one-half that parallel to $\mathbf{v}_d$. This was called "the continuity effect" by Csanady (1963). For the purpose of future comparison, it is worth pointing out that Csanady's relations imply that

$$\frac{v_{10}}{v_{30}} = \frac{v_{20}}{v_{30}} = 1, \quad \frac{T_{11}}{T_{33}} = \frac{T_{22}}{T_{33}} = \frac{1}{2}, \quad \text{if } \frac{v_g}{u_0} \to \infty, \ \tau_a = 0, \qquad (1.4)$$

where v_{i0} and T_{ii} are ith component of the particle rms fluctuating velocity and ith component of the particle Lagrangian integral time scale, respectively; τ_a is the particle aerodynamic response time [see Eq. (2.1) for detailed definition]. Therefore, the difference between $\epsilon_{11}^p(\infty)$ and $\epsilon_{33}^p(\infty)$ is totally realized through the difference between T_{11} and T_{33}. The conditions of small inertia and large drift velocity can be found in atmospheric flows but are seldom found in industrial flows.

One of the most comprehensive solutions for heavy particle dispersion was done by Reeks (1977) using the second-order iteration approximation. He incorporated both the effect of finite particle inertia and the effect of drift velocity. In the absence of drift velocity, Reeks clearly pointed out that the problem of whether the long-time dispersion coefficient of heavy particles is greater or less than that of the fluid element diffusion coefficient depends on whether the fluid Eulerian integral time scale, T_{mE}, is greater or less than the fluid Lagrangian integral time scale, T_L. The effect of inertia is then related to the Eulerian–Lagrangian problem of turbulence (Lumley 1962; Kraichnan 1964). Heavy particles disperse faster than fluid elements due to inertia in Reeks' analysis since T_{mE} is larger than T_L for the Gaussian random velocity field he used. The relationship between T_{mE} and T_L is also discussed in a recent paper by Wang and Stock (1988). Pismen and Nir (1978) reported a comprehensive analysis based on the independence approximation, which, as noted by Lundgren and Pointin (1976) and Weinstock (1976), is closely related to the second-order iteration approximation.

One obvious disadvantage of Reeks's and Pismen and Nir's analyses is that their results are given as either

integral equations (Reeks) or integro–differential equations (Pismen and Nir). The mathematical complexity makes it difficult to see the importance of various parameters. In view of the need for Lagrangian particle dispersion statistics for both numerical modeling (Picart et al. 1986; Walklate 1986, 1987) and to interpret experimental results (Ferguson 1986; Wang 1990), a mathematically simple but physically realistic relationship for heavy particle dispersion is needed.

In this work, we develop an algebraic equation for the dispersion of heavy particles in terms of measurable flow Eulerian scales, particle inertia, and particle drift velocity. We start by relating the particle velocity correlation tensor to the fluid velocity correlation tensor at the points lying on the particle trajectory. The fluid velocity correlation along the particle trajectory is then related to fluid Eulerian velocity correlations and fluid Lagrangian velocity correlation by including the effects of inertia and drift velocity. This step is similar to Csanady's (1963) analysis, except we allow the time scale of fluid velocity correlation seen by the heavy particle in the absence of drift velocity to be a function of particle inertia. Combining the above relations, we find the particle Lagrangian velocity correlation, the rms fluctuating velocity, and integral time scale in terms of three dimensionless parameters; the Stokes number, the drift parameter, and the turbulence structure parameter.

Detailed interpretations of the results follow. They include discussions of the shape of the particle Lagrangian velocity correlation, dispersion statistics under three asymptotic cases in the inertia-drift parameter domain, and the importance of the coupling of the inertia and the drift velocity. The relative roles of inertia and drift velocity on the dispersion coefficient are examined to clarify the question of whether heavy particles disperse more or less than the fluid elements. The inclusion of nonlinear drag into the analysis is also made possible. Finally, the results of the analysis are compared with numerical simulation (Wang 1990) and other analyses (Reeks 1977; Csanady 1963). Previous "contradictory" particle dispersion data (Arnason 1982) can now be explained as a result of different combinations of the inertia parameter and the drift parameter.

2. Analysis

We consider the motion of heavy spherical particles in a uniform, isotropic, stationary, and homogeneous turbulent flow. The particle is assumed to be small in comparison with the Kolmogoroff microscale of the turbulence, and the loading dilute enough that the presence of the particles does not modify the turbulence structure. On the other hand, the particle is considered to be much larger than the fluid molecules and to have an aerodynamic response time much larger than the mean molecular collision time so that the effect of Brownian motion can be neglected in comparison to the dispersion by turbulent eddies. Since in grid-generated turbulent flow of air (Snyder and Lumley 1971) the Kolmogoroff microscale is in the range of 300–700 μm, the above assumptions are applicable to the dispersion of particles in the size range of 10–100 μm. Further, since the dispersion of heavy particles is mainly governed by the turbulent motion of the energy-containing eddies, of typical size 2–5 cm (Snyder and Lumley 1971), the same assumptions can be used, as a first-order approximation, to the dispersion of particles as large as 1 mm.

The aerodynamic response time, τ_a, for a particle is defined as

$$\tau_a = \frac{\rho_p d_p^2}{18\mu}, \tag{2.1}$$

where ρ_p is the mass density of the particle, d_p is the diameter of the particle, and μ is the dynamic viscosity of the fluid. Here τ_a represents the time necessary for the velocity of a particle injected into a quiescent fluid to reach $1/e$ of its initial value if the drag on the particle is in the Stokes range ($\mathrm{Re}_p < 1$).

The motion of a heavy particle is considered in a frame of reference moving with the mean fluid velocity (moving Eulerian frame). Under the assumption that the density of the particle ρ_p is much larger than the density of the fluid ρ (say, $\rho_p/\rho \geq 100$), the BBO (Basset–Boussinesq–Oseen) equation of motion (Maxey and Riley 1983) reduces to the following form:

$$\frac{dV_i(t)}{dt} = \frac{[u_i(\mathbf{Y}(t), t) - V_i(t)]}{\tau_a} f + q\delta_{i3}; \tag{2.2}$$

$$\frac{dY_i(t)}{dt} = V_i(t), \tag{2.3}$$

where $V_i(t)$ and $Y_i(t)$ are the velocity and the location of a heavy particle, respectively; q is the body force per unit mass acting on the particle due to gravity or electrostatic forces and is considered to be a constant. The "3" direction is aligned with the body force vector; $u_i(\mathbf{x}, t)$ is the fluid Eulerian velocity, which for our case, has a zero mean value everywhere, $\langle u_i(\mathbf{x}, t)\rangle = 0$.

We start by assuming the drag force acting on a particle as it moves through the flow is linear (Stokes drag); that is, the f factor in (2.2) is set to 1. In this case, the drift velocity of a particle in a quiescent fluid is

$$v_d = \tau_a q. \tag{2.4}$$

Stokes drag is valid when the particle Reynolds number is much less than one. Due to the finite drift velocity, however, the particle Reynolds number can often be larger than one. In general, an empirical nonlinear drag

should be used with heavy particles. This may be included by letting f be a function of the particle Reynolds number. A nonlinear drag applicable for a wide range of particle Reynolds number will be considered in section 3d. When nonlinear drag is introduced, the particle response time and the drift velocity will be less than those given by (2.1) and (2.4) by a factor of f^{-1}.

Since the fluid velocity at the location of the heavy particle, $u_i^p(t) \equiv u_i(\mathbf{Y}(t), t)$, is an unknown nonlinear function of the particle location, $\mathbf{Y}(t)$, and $\mathbf{Y}(t)$ is determined by the time history of the particle velocity; $\mathbf{V}(t)$, (2.2), and (2.3) constitute a nonlinear dynamic system and have no exact solution. The particle velocity, however, is not of direct interest to us. The second moment of the particle velocity, that is, the velocity correlation tensor,

$$R_{ij}^p(\tau) = \langle v_i(t)v_j(t+\tau)\rangle, \tag{2.5}$$

is sufficient to determine the dispersion statistics. The aim of our analysis is to relate this correlation to the inertia, the drift velocity, and the measurable fluid Eulerian statistics.

a. Lagrangian velocity correlation of heavy particles

In this section, a relation between the particle velocity correlation, $R_{ij}^p(\tau)$, and the fluid velocity correlation seen by a heavy particle; namely,

$$R_{ij}^f(\tau) \equiv \langle u_i^p(0)u_j^p(\tau)\rangle = \langle u_i(\mathbf{Y}(0), 0)u_j(\mathbf{Y}(\tau), \tau)\rangle, \tag{2.6}$$

is developed. Since the long-time dispersion statistics are of interest to us, we assume that the particle has been moving in the turbulent flow for a long time so that it reaches a state of dynamic equilibrium with the flow. The particle velocity can be found by integrating (2.2) to give (Reeks 1977)

$$V_i(t) = \int_{-\infty}^{t} \frac{u_i(\mathbf{Y}(\tau), \tau)}{\tau_a} \exp\left(\frac{\tau - t}{\tau_a}\right) d\tau + v_d\delta_{i3}. \tag{2.7}$$

Maxey (1987) has shown that the mean drift velocity of a particle is slightly larger than v_d (less than 3% $\sim$ 5% in most cases). If this slight difference is neglected, the instantaneous fluctuating velocity of the particle is $v_i(t) \equiv V_i(t) - \langle V_i(t)\rangle = V_i(t) - v_d\delta_{i3}$. Combining (2.5), (2.6), and (2.7), we obtain

$$R_{ij}^p(\tau) = \frac{1}{\tau_a^2}\int_{-\infty}^{0}\int_{-\infty}^{\tau} R_{ij}^f(\tau_1 - \tau_2) \times \exp\left(\frac{\tau_1 + \tau_2 - \tau}{\tau_a}\right) d\tau_1 d\tau_2. \tag{2.8}$$

Partial integration of Eq. (2.8) gives

$$\begin{aligned} R_{ij}^p(\tau) &= \frac{1}{2\tau_a}\int_{-\infty}^{\infty} \exp\left(-\frac{|\zeta - \tau|}{\tau_a}\right) R_{ij}^f(\zeta)\, d\zeta \\ &= \frac{1}{2\tau_a}\int_{-\infty}^{\tau} \exp\left(\frac{\zeta - \tau}{\tau_a}\right) R_{ij}^f(\zeta)\, d\zeta \\ &\quad + \frac{1}{2\tau_a}\int_{-\infty}^{-\tau} \exp\left(\frac{\zeta + \tau}{\tau_a}\right) R_{ij}^f(\zeta)\, d\zeta. \end{aligned} \tag{2.9}$$

This relation shows the difference between the particle velocity correlation and the fluid velocity correlation realized along a particle's trajectory. The difference is due to the particle inertia (finite τ_a). Equation (2.9) is essentially the same as Eq. (2.13) in Reeks' (1977) paper, except the latter uses the notation of the step function. In Csanady's (1963) analysis, he assumed $R_{ij}^p(\tau) = R_{ij}^f(\tau)$, which is true only when $\tau_a \to 0$. Consequently, Csanady's results are only good for zero-inertia particles. Many interesting phenomena are lost when inertia is neglected.

Equation (2.9) can also be obtained by first taking Fourier transform of the equation of motion, (2.2), to relate the power spectrum of $v_j(t)$ to the power spectrum of $u_j^p(t)$ (Hinze 1975), and then performing the reverse Fourier transform.

From (2.9), we can clearly see the "smoothing" effect of the inertia on $R_{ij}^p(\tau)$. Here $R_{ij}^f(\tau)$ is smoothed by a symmetric weighting function, $\exp\{-[(\zeta - \tau)/\tau_a]\}/(2\tau_a)$, to give $R_{ij}^p(\tau)$. As a result, the particle turbulence energy,

$$v_{i0}^2 \equiv R_{ii}^p(0), \tag{2.10}$$

will be less than the fluid turbulence energy, $u_0^2 \equiv R_{11}^f(0) = R_{22}^f(0) = R_{33}^f(0)$. [No summation is assumed for the repeated index i in (2.10) and future equations.] The reduction of particle turbulence energy with increasing τ_a is a natural result of the inability of the particle to respond to the high-frequency fluid oscillations. On the other hand, the particle integral time scale,

$$T_{ii} = \int_0^{\infty} \frac{R_{ii}^p(\tau)}{R_{ii}^p(0)}\, d\tau, \tag{2.11}$$

is larger than the fluid integral time scale along the particle's trajectory, T_{ii}^f. Integrating both sides of (2.9) with respect to τ from 0 to ∞ gives the following identity:

$$T_{ii}v_{i0}^2 = T_{ii}^f u_0^2. \tag{2.12}$$

The left-hand side of (2.12) is the long-time particle diffusivity. Tchen (1947) ignored the difference between T_{ii}^f and the fluid Lagrangian integral time T_L, which led him to the false conclusion that the long-time particle diffusivity is equal to the long-time fluid diffusivity. Gouesbet et al. (1984) found that the short-time particle diffusivity is larger than the fluid diffu-

sivity if the fluid Lagrangian velocity correlation is assumed to have a negative loop. Unfortunately, they also assumed $T_{ii}^f = T_L$. In fact, even in the case of zero drift velocity, T_{ii}^f is substantially different from T_L and is related to the particle's inertia parameter. The effect of the inertia on T_{ii}^f is the major reason the particle diffusivity can be larger than the fluid diffusivity.

Equation (2.9) does not solve our problem, since $R_{ij}^f(\tau)$ is still unknown. The important effect of crossing trajectories and the additional effect of inertia on the particle velocity correlation $R_{ij}^p(\tau)$ is embedded in the fluid velocity correlation seen by a heavy particle—$R_{ij}^f(\tau)$.

b. *The fluid velocity correlation seen by a heavy particle*

To relate $R_{ij}^f(\tau)$ to the statistics of fluid turbulence, we adopt the idea of Csanady (1963) but include the effect of inertia. More complicated analyses for $R_{ij}^f(\tau)$ were done by Reeks (1977), Pismen and Nir (1978), and Mei and Adrian (1989). However, the mathematical complexities make it difficult to apply their results to a parametric study. In addition, they assume the turbulence was a Gaussian random field with a specific form for the fluid velocity correlations. The beneficial feature of our analysis is that the final results will be in algebraic equations rather than integral or integro–differential equations.

In this study we focus on the long-term dispersion statistics. The general physical consideration here is that the long-term dispersion of heavy particles is dominated by the large-scale turbulent motions where most of the turbulent kinetic energy is located. In such a context, the integral or outer scales of the fluid motion is of importance. We start by assuming all the normalized velocity autocorrelations of the turbulent flow in the moving Eulerian frame to be exponential functions; namely,

$$D_L(\tau) = \exp(-|\tau|/T_L) \tag{2.13a}$$

$$D_{mE}(\tau) = \exp(-|\tau|/T_{mE}) \tag{2.13b}$$

$$f(r) = \exp(-|r|/L_f) \tag{2.14a}$$

$$g(r) = \left(1 - \frac{|r|}{2L_f}\right)\exp(-|r|/L_f), \tag{2.14b}$$

where $D_L(\tau)$ is the fluid Lagrangian velocity correlation, $D_{mE}(\tau)$ is the one-point fluid Eulerian velocity correlation, and $f(r)$ and $g(r)$ are the longitudinal and transverse fluid spatial velocity correlations, respectively; T_L is the fluid Lagrangian integral time scale, T_{mE} is the fluid Eulerian integral time scale, and L_f is the fluid spatial integral length scale. We must note that T_{mE} is measured in a frame moving with the field mean velocity of the flow, while most atmospheric data of Eulerian time scale are taken from fixed stations (see Pasquill and Smith 1983). A fundamental distinction should be made between the time scale in a moving frame and that in a fixed frame, as pointed out by Wang and Stock (1988). The assumed exponential form may not be the best choice, but it is the value of integral scales not the shape of velocity correlations that is our concern in the present context. In fact, Wang (1990) showed that the shape of the correlations has little effect on the long-term dispersion statistics. Equations (2.14a) and (2.14b) satisfy the continuity relation for isotropic turbulence:

$$g(r) = f(r) + \frac{r}{2}\frac{df}{dr}. \tag{2.15}$$

Exponential correlations are easy to use: they fit the experimental data (Hinze 1975, p. 253) and have desirable properties related to turbulent diffusion in the inertia subrange (Tennekes 1979).

Among the fluid turbulence scales, T_L is most difficult to obtain experimentally because it requires measurements following the random motion of fluid elements. Nevertheless, some useful data have been obtained by Snyder and Lumley (1971) and Shlien and Corrsin (1974). More recently, Sato and Yamamoto (1987) measured T_L in grid turbulence by optically tracking small tracer particles. Alternatively, T_L can be related to measurable parameters of the flow, that is, T_{mE}, L_f, and u_0 by either theoretical approximations (Wang and Stock 1988) or direct numerical simulations (Yeung 1989).

Now consider the velocity correlation of the fluid as seen by a heavy particle with time delay τ. The mean spatial displacement in this time interval for a heavy particle will be $v_d\tau$. This displacement is due to the free fall of the particle, since particle motion due to the turbulence will not result in any mean motion. The relative displacement causes a loss of fluid velocity correlation in the neighborhood of the particle and should be reflected in $R_{ij}^f(\tau)$ by including the fluid spatial correlations. In the limiting case of $v_d \to \infty$, or more exactly $L_f/v_d \ll \min(T_L, T_{mE})$, we have $R_{11}^f(\tau) = R_{22}^f(\tau) = g(v_d\tau)$ and $R_{33}^f(\tau) = f(v_d\tau)$.

On the other hand, when the drift velocity vanishes, the trajectory of a heavy particle depends on the magnitude of τ_a, and so does the fluid velocity correlation seen by the particle. We introduce T as the fluid integral time scale seen by a heavy particle in the absence of the drift velocity. Then T is a function of the particle inertia. In Csanady's (1963) work, T was equal to T_L because he assumed zero inertia.

In general, when both the inertia and the drift velocity are nonzero, their effects can be included in $R_{ij}^f(\tau)$ by the hypothesis of Csanady that $R_{33}^f(\tau)$ is constant on the ellipses

$$\frac{\tau^2}{T^2} + \frac{v_d^2\tau^2}{L_f^2} = \text{const.} \tag{2.16}$$

This hypothesis ensures a smooth transition of $R_{ij}^f(\tau)$ from fluid temporal velocity correlation (of a time scale T) to fluid spatial velocity correlation when the drift velocity increases from 0 to ∞. Using (2.16) and the velocity correlations (2.13a,b) and (2.14a,b), we obtain the fluid velocity correlation seen by a heavy particle as

$$R_{11}^f(\tau) = R_{22}^f(\tau) = u_0^2\left[1 - \frac{v_d\tau}{2L_f}\right]\exp\left\{-\frac{\tau}{T}\sqrt{1 + m_T^2\gamma^2}\right\}, \quad (2.17)$$

$$R_{33}^f(\tau) = u_0^2\exp\left\{-\frac{\tau}{T}\sqrt{1 + m_T^2\gamma^2}\right\}, \quad (2.18)$$

where the dimensionless parameters are

$$\gamma = v_d/u_0 = \tau_a q/u_0, \quad (2.19)$$

$$m_T \equiv Tu_0/L_f = m\frac{T}{T_{m\mathrm{E}}}, \quad (2.20a)$$

where

$$m = T_{m\mathrm{E}}u_0/L_f; \quad (2.20b)$$

m can be called the turbulence structure parameter, since it is the ratio of one-point eddy decay time $T_{m\mathrm{E}}$ to the eddy turnover time L_f/u_0. A reasonable value for m is of order one, but it may vary between 0.1 and 10 for different flows. We also introduce a Stokes number based on T for later use,

$$\mathrm{St}_T \equiv \tau_a/T = \mathrm{St}\times\frac{T_{m\mathrm{E}}}{T}, \quad (2.21a)$$

where St is the normal Stokes number and a measure of the relative importance of the particle's inertia,

$$\mathrm{St} = \tau_a/T_{m\mathrm{E}}. \quad (2.21b)$$

Now we have all the information necessary to find the particle Lagrangian velocity correlation.

c. *The general results*

Substituting (2.17) or (2.18) into (2.9) and after lengthy manipulation, we obtain the particle Lagrangian velocity correlation

$$R_{11}^p(\tau) = \frac{u_0^2}{\theta}\exp\left(-\frac{\tau}{\tau_a}\right)\left\{\mathrm{St}_T\sqrt{1 + m_T^2\gamma^2} - 0.5\gamma m_T\mathrm{St}_T\frac{\mathrm{St}_T^2(1 + m_T^2\gamma^2) + 1}{\theta}\right\} + \frac{u_0^2}{\theta}\exp\left[-\sqrt{1 + m_T^2\gamma^2}\,\frac{\tau}{T}\right]\times\left\{-1 + \frac{m_T\mathrm{St}_T^2\gamma\sqrt{1 + m_T^2\gamma^2}}{\theta} + 0.5m_T\gamma\frac{\tau}{T}\right\} \quad (2.22)$$

$$R_{33}^p(\tau) = \frac{u_0^2\mathrm{St}_T\sqrt{1 + m_T^2\gamma^2}}{\theta}\exp\left(-\frac{\tau}{\tau_a}\right) - \frac{u_0^2}{\theta}\exp\left[-\sqrt{1 + m_T^2\gamma^2}\,\frac{\tau}{T}\right], \quad (2.23)$$

where $\theta \equiv \mathrm{St}_T^2(1 + m_T^2\gamma^2) - 1$. These equations have two removable singular points, one at $\tau_a = 0$ and the other at $\theta = 0$. When $\tau_a = 0$, (2.22) and (2.23) can be reduced to

$$R_{11}^p(\tau) = u_0^2\exp\left[-\sqrt{1 + m_T^2\gamma^2}\,\frac{\tau}{T}\right]\times\left\{1 - 0.5m_T\gamma\frac{\tau}{T}\right\}, \quad (2.22a)$$

$$R_{33}^p(\tau) = u_0^2\exp\left[-\sqrt{1 + m_T^2\gamma^2}\,\frac{\tau}{T}\right]. \quad (2.23a)$$

When $\theta = 0$, that is, $\mathrm{St}_T^2(1 + m_T^2\gamma^2) = 1$, (2.22) and (2.23) become

$$R_{11}^p(\tau) = u_0^2\exp\left(-\frac{\tau}{\tau_a}\right)\times\left\{\frac{3 + \mathrm{St}_T}{8} + \frac{3 + \mathrm{St}_T}{8}\frac{\tau}{\tau_a} - \frac{1 - \mathrm{St}_T}{8}\left(\frac{\tau}{\tau_a}\right)^2\right\}, \quad (2.22b)$$

$$R_{33}^p(\tau) = \frac{u_0^2}{2}\exp\left(-\frac{\tau}{\tau_a}\right)\left\{1 + \frac{\tau}{\tau_a}\right\}. \quad (2.23b)$$

To study the long-time dispersion characteristics, we need the particle long-time dispersion coefficient, the particle velocity scale, and the particle integral time scale. All of them are obtainable from the above velocity correlations. The particle velocity scale is equal to $\sqrt{R_{ii}^p(0)}$. The ratio of the particle rms velocity to the fluid rms velocity can be written as

$$v_{10}/u_0 = v_{20}/u_0 = \left(\frac{1}{1 + \mathrm{St}_T\sqrt{1 + \gamma^2 m_T^2}} - \frac{0.5m_T\gamma\mathrm{St}_T}{(1 + \mathrm{St}_T\sqrt{1 + \gamma^2 m_T^2})^2}\right)^{1/2}, \quad (2.24)$$

$$v_{30}/u_0 = \left(\frac{1}{1 + \mathrm{St}_T\sqrt{1 + \gamma^2 m_T^2}}\right)^{1/2}. \quad (2.25)$$

Noting the definition (2.5), we can substitute (2.22) or (2.23) into (1.1) to derive the particle long-time dispersion coefficients. When normalized by u_0^2T, we obtain

$$\frac{\epsilon_{11}^p(\infty)}{u_0^2T} = \frac{\epsilon_{22}^p(\infty)}{u_0^2T} = \frac{\sqrt{1 + m_T^2\gamma^2} - 0.5m_T\gamma}{1 + m_T^2\gamma^2}, \quad (2.26)$$

$$\frac{\epsilon_{33}^p(\infty)}{u_0^2T} = \frac{1}{\sqrt{1 + m_T^2\gamma^2}}. \quad (2.27)$$

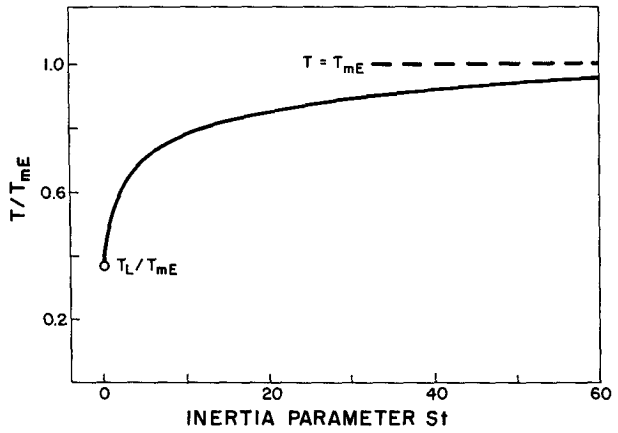

FIG. 1. The time scale of turbulence seen by a heavy particle of zero drift as a function of particle's inertia from a numerical simulation.

It follows that the normalized particle integral time scales are

$$\frac{T_{11}}{T} = \frac{T_{22}}{T} = \frac{\epsilon_{11}/u_0^2 T}{(v_{10}/u_0)^2}$$

$$= \frac{(\sqrt{1 + m_T^2\gamma^2} - 0.5m_T\gamma)(1 + \mathrm{St}_T\sqrt{1 + \gamma^2 m_T^2})^2}{(1 + m_T^2\gamma^2)(1 + \mathrm{St}_T\sqrt{1 + m_T^2\gamma^2} - 0.5m_T\gamma\mathrm{St}_T)} \quad (2.28)$$

$$\frac{T_{33}}{T} = \frac{\epsilon_{33}/u_0^2 T}{(v_{10}/u_0)^2} = \frac{1 + \mathrm{St}_T\sqrt{1 + m_T^2\gamma^2}}{\sqrt{1 + m_T^2\gamma^2}}. \quad (2.29)$$

Before discussing these results, we should clarify how the time scale T is related to the particle's inertia.

d. *The fluid time scale seen by a heavy particle of zero drift*

Physically, the fluid time scale seen by a heavy particle with zero drift is T_{mE} in the limit that $\mathrm{St} \gg 1$, since in this situation the heavy particle responds slowly to the fluid oscillations and essentially stays at one point during a period of time of the order T_{mE}. On the other hand, $T = T_L$ if $\mathrm{St} \to 0$; that is, the heavy particle reduces to a fluid element. Therefore, in general, T is a function of St and varies between T_L and T_{mE}. The amount T changes with St depends on the difference between the fluid Lagrangian scale T_L and the fluid Eulerian scale T_{mE}. Experimental data of Sato and Yamamoto (1987) suggest that $T_L = 0.3 \sim 0.6T_{mE}$ for a grid-generated turbulence. An analytical approximation (Wang and Stock 1988) for Gaussian random turbulence concludes that T_L/T_{mE} is always less than one and that it is a function of the structure parameter m. A numerical simulation of Wang and Stock (1992) gives $T_L = 0.356T_{mE}$ when $m = 1$. Recent direct numerical simulation (Yeung 1989) also found that the Lagrangian integral time, T_L, is less than the Eulerian integral time, T_{mE}. These results imply that T_L is different from T_{mE} and thus T must be considered as a function of St.

A numerical simulation using turbulence generated by Fourier modes (Wang and Stock 1992) was done to determine how T changed with St for $m = 1$. The result is shown in Fig. 1: T increases quickly with St when St is small, but gradually approaches T_{mE} when St becomes large. A good curve fit to the numerical results is

$$\frac{T(\mathrm{St})}{T_{mE}} = 1. - \frac{0.644}{(1 + \mathrm{St})^{0.4(1+0.01\mathrm{St})}}, \quad (2.30)$$

where the constant $0.644 = 1 - T_L/T_{mE}$. This semi-empirical relation for T, although not general, is used later in this analysis. Using Eq. (2.30), T_{mE}, a constant based only on the Eulerian flow field, can be used to replace T in the results of section 2c.

In summary, we now have algebraic equations for the long-time dispersion statistics of heavy particles in terms of three measurable dimensionless parameters: m, St, and γ_0.

3. Discussions of the results

Here we present detailed discussions of the analytical results with an emphasis on the phenomena that were not realized by earlier investigators. Physical explanations, whenever possible, are provided to support the analytical findings.

a. *The shape of particle Lagrangian velocity correlations*

A knowledge of how the shape of the velocity correlation $R_{ij}^p(\tau)$ changes with the physical parameters is essential for understanding particle dispersion. Sets of contour plots for both the vertical velocity correlation, (2.22), and the horizontal velocity correlation, (2.23), normalized by the respective velocity scale given by (2.24) or (2.25), are shown in Figs. 2, 3, and 5. In these plots, the x axis is the dimensionless time delay τ/T_{mE} and the y axis is the drift parameter γ, and the curves represent lines of constant correlation. A turbulence structure parameter, m, of one was used in these plots. Inertia parameter St varies from plot to plot. Because the parameter m_T (or m) and the parameter γ are always grouped together in (2.22) and (2.23), it is sufficient to consider only $m = 1$. The effect of increasing m is equivalent to the effect of decreasing γ, since physically the reduction of the Eulerian spatial length scale L_f has the same effect as the increase of drift velocity v_d, for example, enhancing the effect of the crossing trajectories.

1) THE HORIZONTAL VELOCITY CORRELATION $R^p_{11}(\tau)$ OR $R^p_{22}(\tau)$

The left side of Fig. 2 shows a typical contour plot for the horizontal correlation $R^p_{11}(\tau)$ in the $\gamma - \tau/T_{mE}$ plane with St = 0.2. Each contour represents a fixed value for the correlation $R^p_{11}(\tau)$. A horizontal cut gives the usual correlation curve at one drift velocity (on the right). The negative correlation region for the particle horizontal correlation shows an interesting behavior with increasing γ. The negative correlation originates from the negative loop in the fluid transverse correlation $g(r)$. No negative correlation exists for $\gamma = 0$. For small γ, the negative correlation region increases as γ increases. As γ continues to increase, however, the negative region will eventually disappear for this small inertia situation. Physically, this phenomenon is a result of the competition between the effect of inertia (with the time scale τ_a) and the effect of drift velocity (with the time scale L_f/v_d). For a given St, no matter how small, the inertia will eventually govern the time scale of the horizontal correlation as the drift parameter becomes arbitrarily large; that is, a state of $L_f/v_d < \tau_a$ will be reached. This dramatic sensitivity of the correlation shape or scale to the inertia, when the drift parameter is sufficiently large, is a result of the coupling effect of the inertia and the drift. This coupling was not realized in Csanady's (1963) analysis. The coupling effect is seen when

$$\mathrm{St}\gamma m = \frac{\tau_a v_d}{L_f} > 1. \tag{3.1}$$

Further, the negative correlation zone in the $\gamma - \tau/T_{mE}$ plane shrinks as the inertia increases (Fig. 3). It eventually disappears when St is sufficiently large. The minimum values of the horizontal velocity correlation are shown as a function of the inertia in Fig. 4. The minimum value increases with St and is zero (no negative correlation zone) when St $\geqslant$ 1.

2) THE VERTICAL VELOCITY CORRELATION $R^p_{33}(\tau)$

The vertical velocity correlation has a simpler shape than the horizontal correlation because there is no negative correlation zone. Contour plots of the vertical correlation (Fig. 5) show that the isopleth lines are essentially vertical and become less dependent on the drift parameter as the inertia parameter becomes large. As a particle with large inertia moves through the flow, the time scale of the fluid velocity seen by it is relatively small. The motion of a heavy particle in this instance is analogous to Brownian motion and the equation of motion is similar to the Langevin equation (Csanady 1973). Consequently, the normalized velocity correlations in both the horizontal and the vertical directions are

$$\frac{R^p_{ii}(\tau)}{R^p_{ii}(0)} = \exp\left(-\frac{\tau}{\tau_a}\right) \approx \exp\left(-\frac{\tau}{T_{mE}}\cdot\frac{1}{\mathrm{St}}\right); \quad \text{if} \quad \tau_a \gg \min\left(T_{mE}, \frac{L_f}{v_d}\right). \tag{3.2}$$

Therefore, the correlation is mostly governed by the inertia. Actually, the "if" condition is valid even for small St in the case of arbitrarily large drift velocity. This is shown in Figs. 3 and 5.

b. Some asymptotic relations

In this section we consider the long-time dispersion characteristics of particles under three extreme cases

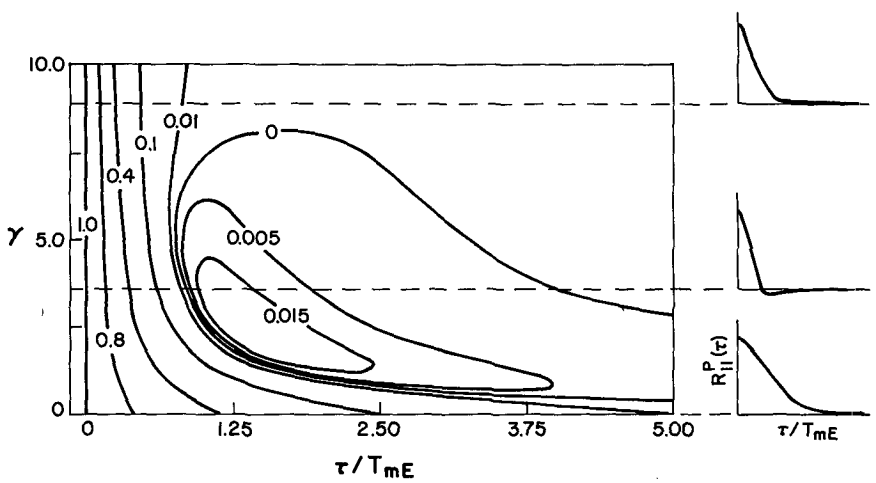

FIG. 2. A contour plot of particle Lagrangian velocity correlation in the direction normal to the drift velocity [$R^p_{11}(\tau)$ or $R^p_{22}(\tau)$] in a $\gamma - \tau/T_{mE}$ plane with St = 0.2 and m = 1.

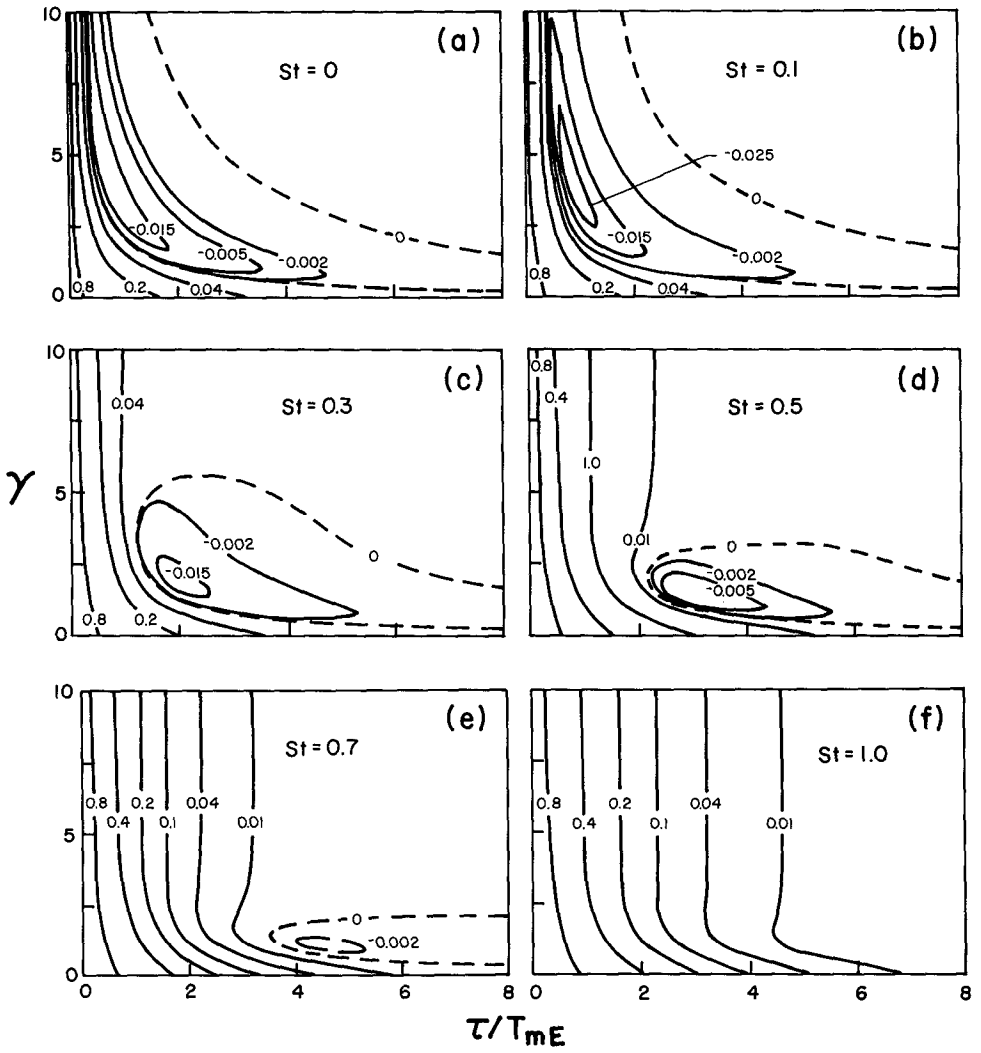

FIG. 3. Contour plots of particle Lagrangian velocity correlation in the horizontal direction [$R^p_{11}(\tau)$ or $R^p_{22}(\tau)$] in a $\gamma - \tau/T_{mE}$ plane with $m = 1$ and different inertia parameters.

for the γ-St combination. For these conditions, the turbulence structure parameter m is assumed to be 1 without loss of generality.

1) $\gamma = 0$

In this case, (2.24) and (2.25) reduce to

$$\frac{v_{10}}{u_0} = \frac{v_{20}}{u_0} = \frac{v_{30}}{u_0} = \frac{1}{\sqrt{1 + \mathrm{St}_T}}; \qquad (3.3)$$

namely, all the velocity scales are the same and they decrease with inertia. The time scale increases with the inertia, following (2.28) and (2.29),

$$T_{11} = T_{22} = T_{33} = T + \tau_a. \qquad (3.4)$$

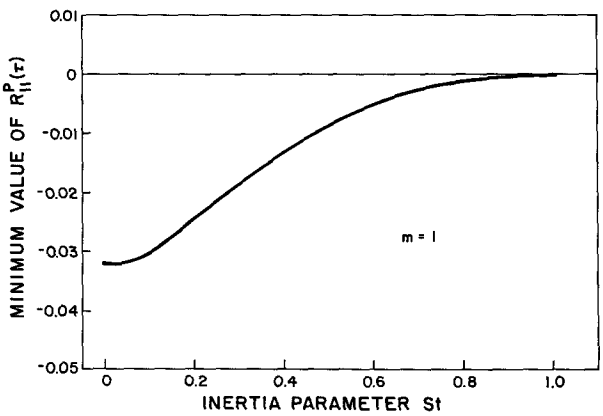

FIG. 4. The minimum value of $R^p_{11}(\tau)$ or $R^p_{22}(\tau)$ on the $\gamma - \tau/T_{mE}$ plane (see Fig. 3) as a function of St.

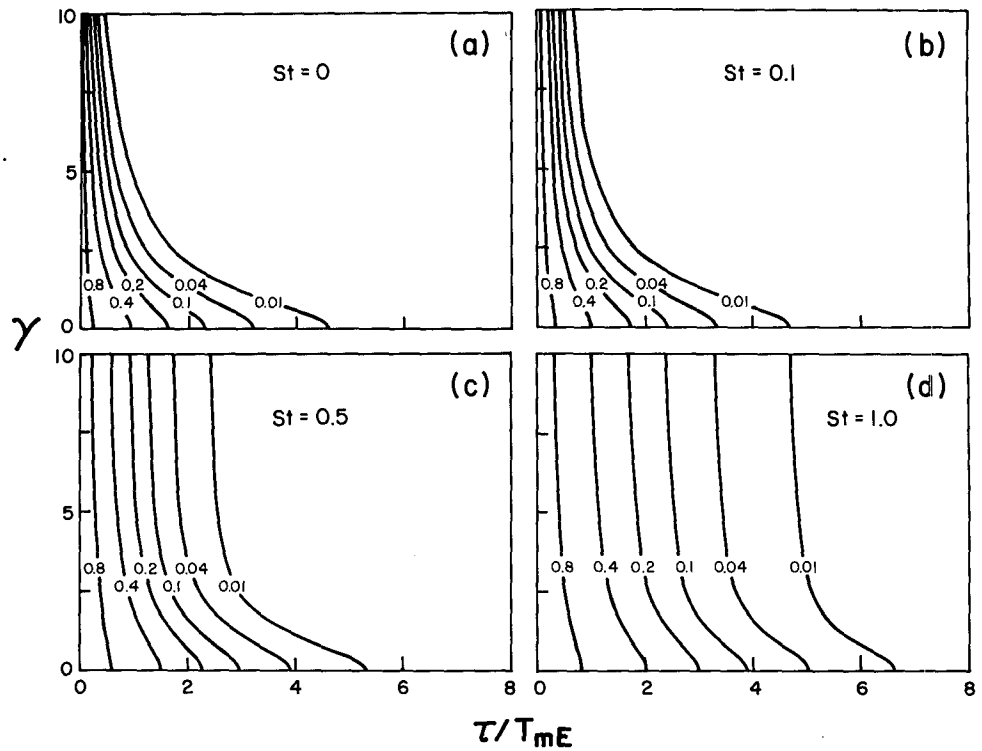

FIG. 5. Contour plots of particle Lagrangian velocity correlation in the vertical direction ($R^p_{33}(\tau)$) in a $\gamma - \tau/T_{mE}$ plane with $m = 1$ and different inertia parameters.

These results show explicitly the "smoothing" effect of the inertia. The net effect of inertia on the particle dispersion coefficient is

$$\epsilon^p_{11}(\infty) = \epsilon^p_{22}(\infty) = \epsilon^p_{33}(\infty) = u_0^2 T(\mathrm{St}). \quad (3.5)$$

Comparing it with the diffusion coefficient of fluid elements, $\epsilon^f(\infty) = T_L u_0^2$, gives

$$\frac{\epsilon^p(\infty)}{\epsilon^f(\infty)} = \frac{T(\mathrm{St})}{T_L}. \quad (3.6)$$

This equation is a special case of the general identity (2.12). Using the relationship for $T(\mathrm{St})$ and noting that $T_L < T_{mE}$, we see that the heavy particles disperse faster than the fluid elements in the absence of a drift velocity. Since the particle velocity fluctuations tend to zero for large inertia, intuition may lead one to the erroneous conclusion that the particle dispersion coefficient approaches to zero under large inertia. The real situation is that the particle Lagrangian time scale tends to infinity in the limit of large inertia time. Since $\epsilon^p_{ii}(\infty) = v^2_{i0} \times T_{ii}$, the dispersion coefficient is of a form $0 \times \infty$, which is finite and equal to $T_{mE} u_0^2$. The ratio $\epsilon^p(\infty)/\epsilon^f(\infty)$ increases with St, and for arbitrarily large inertia, the ratio equals T_{mE}/T_L, as noted by Reeks (1977). According to Sato and Yamamoto (1987), $T_L = 0.3 \sim 0.6 T_{mE}$. Therefore, it is possible for the particle dispersion coefficient to be as much as 100% ~ 200% larger than the fluid diffusion coefficient.

2) St = 0 AND EXTREMELY LARGE γ

For this condition, equations in section 2c reduce to

$$\frac{v_{10}}{u_0} = \frac{v_{20}}{u_0} = \frac{v_{30}}{u_0} = 1.0; \quad (3.7)$$

$$T_{11} = T_{22} = 0.5 \frac{L_f}{v_d}, \quad T_{33} = \frac{L_f}{v_d}; \quad (3.8)$$

$$\epsilon_{11} = \epsilon_{22} = 0.5 u_0^2 L_f / v_d, \quad \epsilon_{33} = u_0^2 L_f / v_d. \quad (3.9)$$

Both the particle dispersion coefficient and the time scale are inversely proportional to the drift velocity. This was first realized by Yudine (1959) and is called the crossing trajectories effect. Also, the horizontal dispersion is half of the vertical dispersion, and this was called the continuity effect by Csanady (1963). The time scale difference, in this zero inertia situation, is totally responsible for the difference between $\epsilon^p_{11}(\infty)$ and $\epsilon^p_{33}(\infty)$.

3) St ≠ 0 AND EXTREMELY LARGE γ ($\gamma \gg 1/\mathrm{St}$)

This is a rather interesting case because it is very close to the zero inertia case, but the time scale and

velocity scale look quite different. In the limit of $St\gamma \gg 1$, Eqs. (2.24) and (2.25) become

$$v_{10} = v_{20} = u_0\left(\frac{0.5}{St_T m_T \gamma}\right)^{1/2} = u_0\left(\frac{0.5 L_f}{\tau_a v_d}\right)^{1/2}, \quad (3.10)$$

$$v_{30} = u_0\left(\frac{1}{St_T m \gamma}\right)^{1/2} = u_0\left(\frac{L_f}{\tau_a v_d}\right)^{1/2}. \quad (3.11)$$

Therefore, the particle turbulence energy is proportional to the fluid correlation time seen by the heavy particle L/v_d, and inversely proportional to the particle aerodynamic response time τ_a. Physically, the oscillating motion of the particle caused by the motion of the neighboring fluid is attenuated by the particle's inertia. From (2.28) and (2.29), the particle time scales are

$$T_{11} = T_{22} = T_{33} = TSt_T = \tau_a. \quad (3.12)$$

This result is also obvious from (3.2). Unlike the particle velocity and time scales, the dispersion coefficients for this case are exactly the same as case 2. The horizontal dispersion coefficient is one-half the vertical dispersion coefficient, and both are inversely proportional to v_g.

In summary, if $\gamma \gg 1/St$, then the difference between the horizontal dispersion and the vertical dispersion, known as the effect of fluid continuity, is due to the difference between the horizontal velocity scale and the vertical velocity scale; that is,

$$\frac{v_{10}}{v_{30}} = \frac{v_{20}}{v_{30}} = \frac{1}{\sqrt{2}}, \quad \frac{T_{11}}{T_{33}} = \frac{T_{22}}{T_{33}} = 1,$$

$$\text{if } \frac{v_g}{u_0} \to \infty, \quad \tau_a \neq 0. \quad (3.13)$$

Comparing (3.13) to (1.4), we see the important role of inertia in determining the particle velocity scale and the particle time scale.

A direct explanation for the direction dependence of the velocity scale shown by (3.10) and (3.11) can be given. For a heavy particle with large drift velocity, the fluid velocity correlation scale seen by the particle in the horizontal direction is half that in the vertical direction since the former is related to the fluid transverse correlation $g(r)$ while the later is related to the fluid longitudinal correlation $f(r)$. In other words, the mean "frequency" for the random force acting on the particle due to the neighboring fluids in the horizontal direction is about twice the mean "frequency" in the vertical direction. Because of the inertia, the particle cannot respond to the fluid motion in the horizontal direction as well as in the vertical direction. This results in larger particle fluctuation energy in the vertical direction.

The above three asymptotic cases show the range of complexity of the dispersion characteristics under more general conditions. First, a combination of case 1 and case 2 suggests that the particle dispersion coefficient can be either larger or less than the fluid diffusion coefficient when both γ and St are finite. Second, due to the fluid continuity, a combination of case 2 and case 3 suggests that not only is the particle vertical dispersion larger than the particle horizontal dispersion but also both the particle velocity scale and time scale in the vertical direction are, in general, larger than those in the horizontal direction. Both these complexities are discussed and clarified in the following section.

c. *The relative roles of inertia and drift velocity*

As shown by the general analytical results given in section 2c, the dispersion process for heavy particles depends on three parameters: St, γ, m. The first two parameters depend on the particle size, density, and fluid scales and the third parameter depends on the fluid turbulence structure. In this section, we shall consider the relative importance of the particle inertia and the drift velocity on the dispersion statistics while holding the structure parameter m fixed at one.

To clearly show the long-time dispersion statistics, we have constructed contour plots, Fig. 6, in a γ–St plane for the particle velocity scales in both the hori-

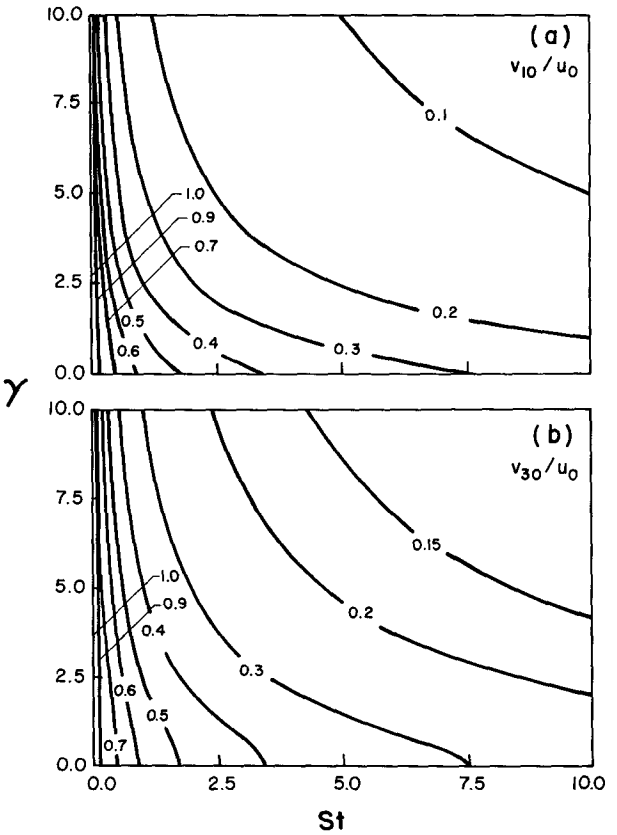

FIG. 6. Contour plots of particle rms fluctuating velocity in the St–γ plane.

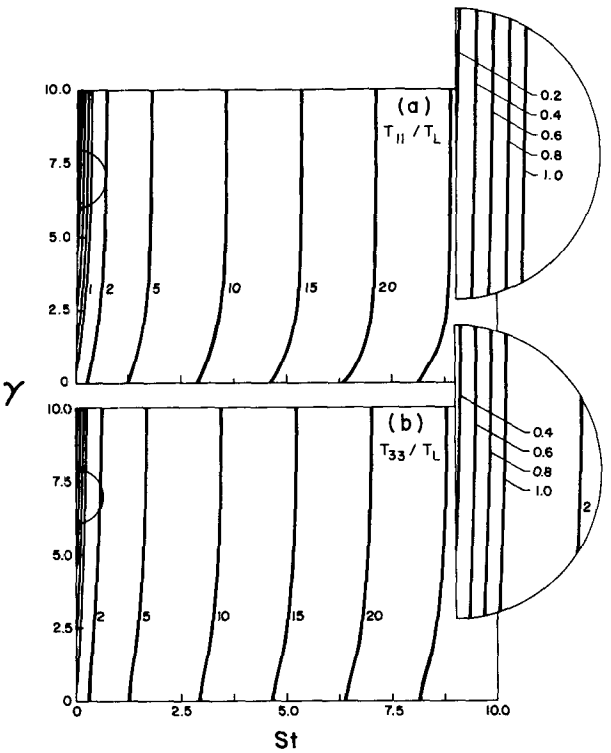

FIG. 7. Contour plots of particle integral time scale in the St–γ plane.

zontal direction and the vertical direction. The particle velocity scales have been normalized by the fluid velocity scale u_0. The particle velocity scale is always less than the fluid velocity scale. The velocity scale ratio, v_{i0}/u_0, is a strong function of St when St is small; that is, contour lines are vertical. As St becomes large, however, the drift velocity has a strong influence on the ratio as well. The dependence of the particle velocity scale upon the drift was not realized in many studies (Meek and Jones 1973; Walklate 1987; Nichols 1990).

Figure 7 shows the particle time scales in both the horizontal direction and the vertical direction, normalized by the fluid Lagrangian scale T_L. The particle time scale is larger than the fluid-diffusion time scale in most of the region. It is mainly a function of the particle's inertia. Only when St is small and γ is large is the particle time scale less than T_L as a result of the crossing trajectories effect.

The question of whether the heavy particles disperse faster or slower than fluid elements is clearly answered by the contour plots for the ratio $\epsilon_{ii}^p(\infty)/\epsilon^f(\infty)$ shown in Fig. 8. The heavy particles disperse faster than the fluid for small value of the drift. The situation is reversed when γ is sufficiently large. The diffusivity ratio, $\epsilon_{ii}^p(\infty)/\epsilon^f(\infty)$, has an upper limit value of T_{mE}/T_L and a lower limit of zero.

The ratio of the fluid diffusivity to the particle diffusivity (particle Schmidt number) has been reported to vary from 0.1 to 2 (Arnason 1984) in various experimental studies. The reason for the wide variation in the particle Schmidt numbers among different experiments can now be explained, by the relative importance of the inertia parameter and the drift parameter in the different experiments. For those measurements involving large inertia parameter but small drift parameter, our analysis suggests that the Schmidt number should be less than one. A Schmidt number larger than 1 goes with those experimental settings that have a large drift parameter. It is worth noting that even if the same heavy particles are used in two experiments, the resulting Schmidt numbers may not agree due to the difference in the fluid turbulence scales [for example, Wells and Stock (1983) versus Arnason and Stock (1986)]. A full account of this interesting issue will be given in a future paper.

So far, we have compared the particle dispersion statistics with the fluid diffusion statistics. In what follows, we compare the particle dispersion statistics in the horizontal direction to those in the vertical direction. Figure 9 shows contour plots for the ratios of the dispersion statistics in the horizontal direction to their respective values in the vertical direction. The three ratios represented by Figs. 9a–c are related by

$$\frac{\epsilon_{11}^p(\infty)}{\epsilon_{33}^p(\infty)} = \frac{v_{10}^2}{v_{30}^2} \times \frac{T_{11}}{T_{33}}. \qquad (3.14)$$

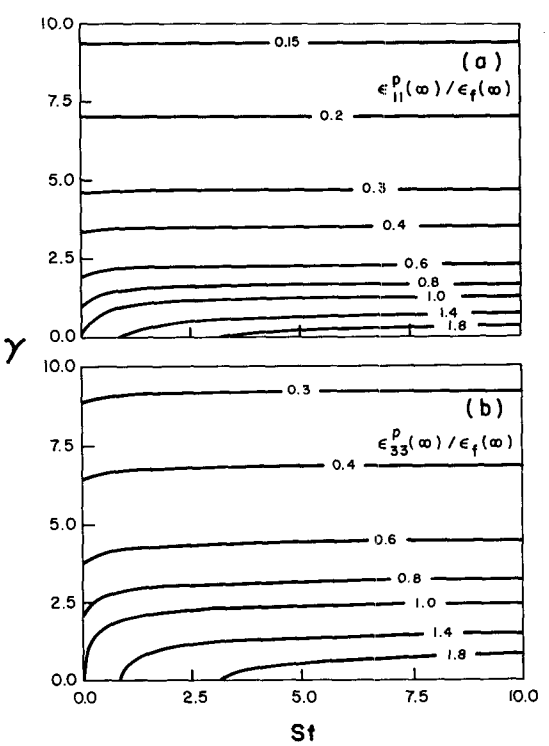

FIG. 8. Contour plots of particle long-time diffusivity in the St–γ plane.

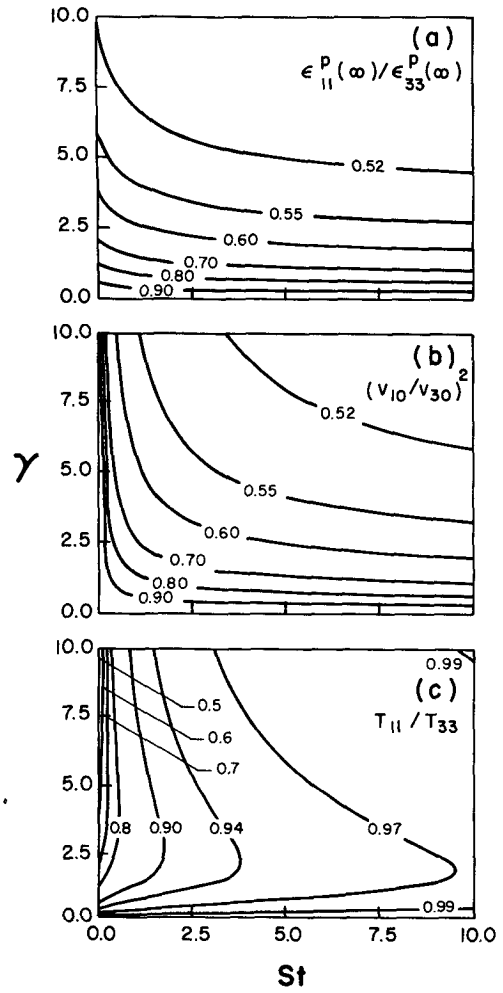

FIG. 9. Contour plots of the diffusivity ratio, velocity scale ratio, and time scale ratio in the St–γ plane.

The effect of fluid continuity on the diffusivity ratio is indicated in Fig. 9a. In section 3b, we showed how the effect of fluid continuity, under the zero inertia limit (St = 0), causes a difference in time scales. On the other hand, for the nonzero inertia case, a difference in the velocity scales results. In general, both v_{10}^2/v_{30}^2 and T_{11}/T_{33} are less than one and vary from 0.5 to 1. This is clearly depicted by Figs. 9b and 9c. Further, using the relation (3.14) and the maps in Fig. 9, we conclude that the diffusivity ratio is mainly controlled by the velocity scale ratio, except in the region of small inertia and large drift.

d. Consideration of nonlinear drag

So far we have assumed that the drag was linear ($f = 1$) in the equations of motion for the heavy particles. This form is good only for a Reynolds number, based on particle size, of less than one. Now we introduce the empirical nonlinear drag law (Rowe 1961). The f factor in (2.2) is given by

$$f = 1 + 0.15\,\mathrm{Re}_p^{0.687}, \tag{3.15a}$$

where the particle Reynolds number is

$$\mathrm{Re}_p = \frac{\rho d_p |\mathbf{V} - \mathbf{u}|}{\mu}. \tag{3.15b}$$

This empirical drag relation is accurate for $\mathrm{Re}_p < 1000$, and has been used in many engineering applications. The readers are warned, though, that the use of quasi-steady nonlinear drag for unsteady flows has not been fully justified and thus is at best as approximation. If the Reynolds number is high enough or the flow velocity varies quickly with time, unsteady vortex shedding will occur in the wake of a spherical particle, while the nonlinear drag is a time-averaged result. In this section, we propose an approximate way to incorporate this drag law into our analysis to extend its applicability. The results will then be compared to the numerical simulation (Wang 1990) in which the same nonlinear drag was used.

If we define effective response time $\tau_e \equiv \tau_a/f$, the equation of motion (2.2) for a heavy particle with nonlinear drag will look the same as the equation of motion for a heavy particle with Stokes drag. In general, the f factor will be a time-dependent random number. We propose to use an effective response time, calculated by the mean value of f; that is, $\tau_e = \tau_a/\bar{f}$. Using nonlinear drag, Wang and Stock (1992) found that the mean drift velocity of a heavy particle in a turbulent flow was very close to the drift velocity in still fluid, v_{d0}. The drift velocity in still flow is given by

$$v_{d0}\left[1 + 0.15\left(\frac{\rho d_p v_{d0}}{\mu}\right)^{0.687}\right] = \tau_a q. \tag{3.16}$$

Therefore, a close approximation for $\bar{f}$ is

$$\bar{f} = 1 + 0.15\left(\frac{\rho d_p v_{d0}}{\mu}\right)^{0.687}. \tag{3.17}$$

Noting that both the inertia parameter and the drift parameter are proportional to the particle response time, we introduce the following effective inertia parameter and the effective drift parameter

$$\mathrm{St}_e = \mathrm{St}/\bar{f} \tag{3.18}$$

$$\gamma_e = \gamma/\bar{f}. \tag{3.19}$$

We hypothesize that the particle dispersion statistics with the nonlinear drag can be reasonably predicted with the analytical results of section 2c if St and γ are replaced by St_e and γ_e, respectively.

We used this hypothesis to obtain the ratio of the particle rms velocities with nonlinear drag to the respective values based on the Stokes drag, and compare the results with those from the numerical simulation (Wang 1990) in Fig. 10. Both the numerical simulation

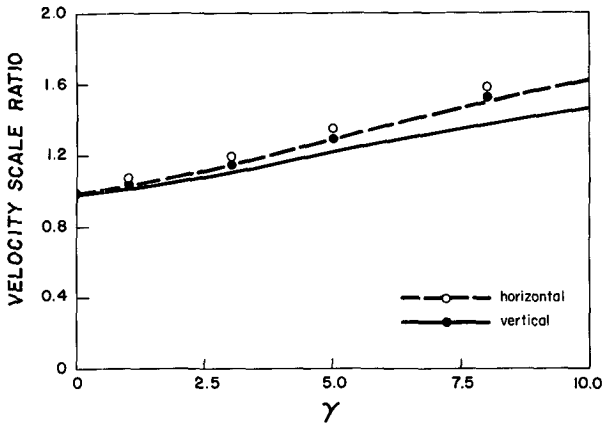

FIG. 10. The ratio of particle rms fluctuating velocity based on the nonlinear drag to the particle rms fluctuating velocity based on the Stokes drag. The symbols represent the simulation results and the lines represent the analytical results.

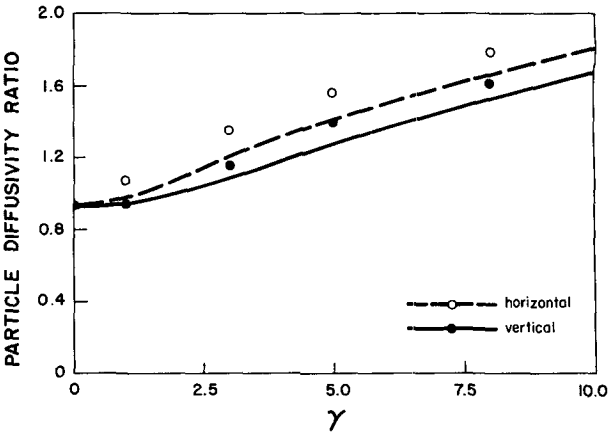

FIG. 11. The ratio of particle diffusivity based on the nonlinear drag to the particle diffusivity based on the Stokes drag. The symbols represent the simulation results and the lines represent the analytical results.

and the proposed analysis show that the particle velocity scale is larger than the equivalent value based on Stokes drag and the ratios increase with the drift parameter. The proposed analysis compares reasonably well with the simulation. The reason for the increase in the velocity scale with a use of the nonlinear drag is mainly that $St_e < St$.

Figure 11 shows the ratio of particle diffusivity to its equivalent value based on the Stokes drag. The proposed analysis is also in good agreement with the simulation, both for predicting larger particle diffusivity when the nonlinear drag is used as compared to the diffusivity based on Stokes drag. The same result has been found earlier by Reeks (1980) using the Eulerian direct interaction technique.

e. Comparison with numerical simulation

In his simulation, Wang (1990) calculates the particle diffusivity, rms fluctuating velocity, and integral time for glass beads of different sizes in a typical nondecaying turbulent flow. He uses random Fourier modes to represent the flow field. This method for kinematic simulations has recently been extended by Fung et al. (1992), and we refer the interested reader to their paper. The same nonlinear drag was included in the simulation. We shall now compare our analysis with the results of the numerical simulation.

Particle diffusivities in both horizontal and vertical directions predicted by the analysis are compared with the results of numerical simulation in Fig. 12. The agreement is very good and the effect of crossing trajectories is clearly seen. Also, the vertical dispersion is consistently larger than the horizontal dispersion due to the effect of fluid continuity.

Figure 13 shows a comparison between the analysis and the simulation for the long-time diffusivity ratio $\epsilon_{11}^p(\infty)/\epsilon_{33}^p(\infty)$, the velocity scale ratio v_{10}^2/v_{30}^2, and the time scale ratio T_{11}/T_{33}. The analysis predicts almost exactly the same value for $\epsilon_{11p}/\epsilon_{33p}$ as the simulation. Reasonable velocity scale ratio and time scale ratio are predicted. Remarkably shown is the change of the time scale ratio with the particle size. It decreases with particle size for $d_p < 60$ μm, but increases with d_p for $d_p > 60$ μm. Such a result is related to the coupling effect of inertia parameter and drift parameter.

f. Comparison with other analyses

Finally, we compare the predictions of this analysis with the analyses given by Csanady (1963) and Reeks (1977). All the analytical results are based on the effective parameters to include the nonlinear drag.

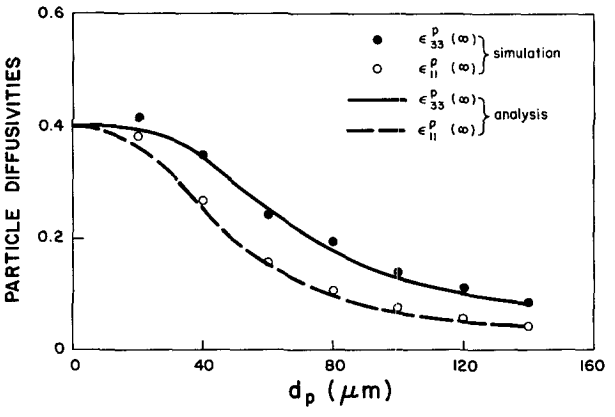

FIG. 12. The diffusivity of glass beads in a typical grid turbulence. ($T_{mE} = 0.225$ s, $u_0 = 11.16$ cm s^{-1}, $m = 1.44$, $T_L/T_{mE} = 0.4$.) The symbols represent the simulation results and the lines represent the analytical results.

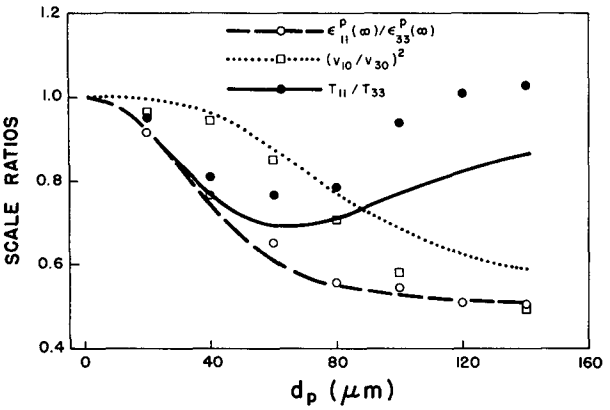

FIG. 13. The diffusivity ratio, rms fluctuating velocity ratio, and integral time scale ratio of glass beads in a typical grid turbulence. The flow parameters are the same as in Fig. 12. The symbols represent the simulation results and the lines represent the analytical results.

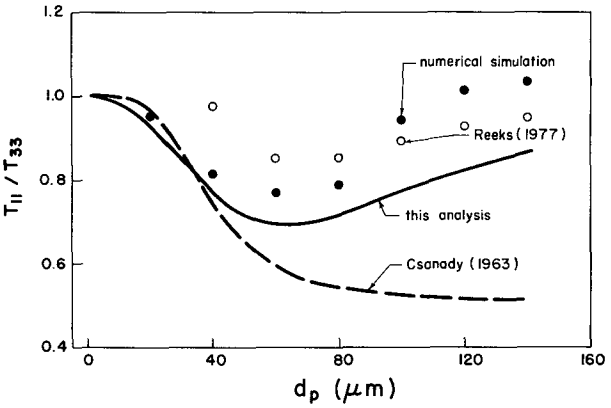

FIG. 15. Comparison of the integral time scale ratio, T_y/T_z.

The square of velocity scale ratio predicted by different analyses and that given by the numerical simulation (Wang 1990) are shown in Fig. 14. A velocity scale ratio of one is assumed for Csanady results because he considered zero inertia particles. Overprediction of the ratio by Reeks' analysis might be due to the difference in the form of velocity correlation and spectrum used by Reeks.

Figure 15 compares the integral time scale ratio predicted by different analyses as well as that given by the numerical simulation. Again, Csanady's analysis deviates from the simulated data at large particle size due to the zero inertia assumption. The present analysis is not as good as Reeks' analysis for large particle size but makes a better prediction for small particle size.

Figure 16 compares the diffusivity ratios. The present analysis agrees with the simulation. Csanady's analysis predicts the diffusivity ratio reasonably well, even if it fails to predict the scale ratios.

All these comparisons are very supportive of our analysis, particularly of its ability to predict the complex behaviors of the velocity scale and time scale.

4. Summary and conclusions

A mathematically simple and physically comprehensive analysis has been developed to relate the dispersion characteristics of heavy particles in a turbulent flow to measurable flow statistics and particle parameters. The analysis accounts for both finite particle inertia and finite particle drift. Also, a nonlinear drag law is incorporated into the analysis to extend its applicability to particles with high slip velocities.

We have shown that heavy particles can disperse faster than fluid elements if the inertia parameter controls the dispersion. The maximum ratio of the particle diffusivity to fluid diffusivity is equal to the ratio of the fluid Eulerian integral time to the fluid Lagrangian integral time. On the other hand, when the drift parameter is much larger than the inertia parameter, the particle diffusivity is less than the fluid diffusivity. This finding can be used to explain previous "contradictory" experimental observations.

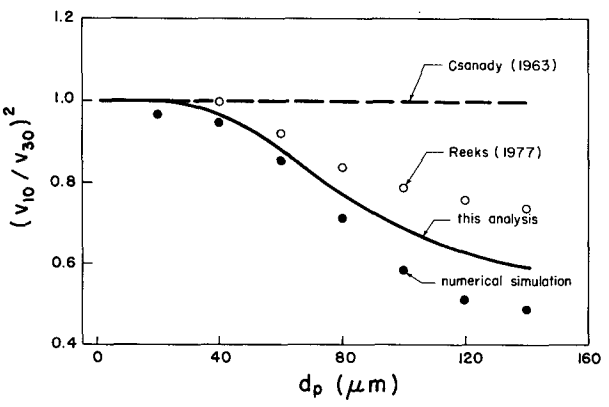

FIG. 14. Comparison of the rms fluctuating velocity ratio, $(v_y/v_z)^2$.

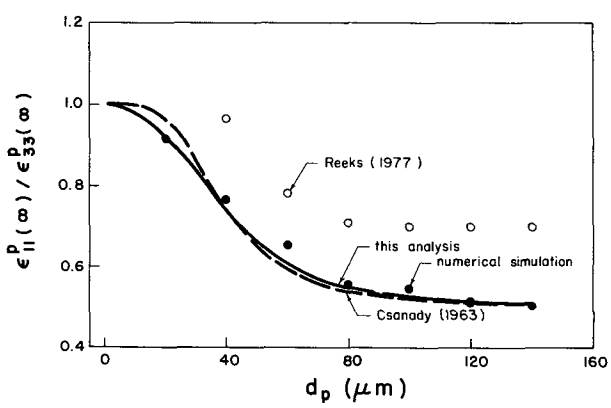

FIG. 16. Comparison of the diffusivity ratio, ϵ_y/ϵ_z.

The coupling effect of the inertia parameter and drift parameter was shown to alter the shape of the particle velocity correlations. It also influences the behavior of the particle velocity scales and time scales. For example, this coupling causes the velocity scale and time scale normal to the drift velocity to be smaller than their respective scales parallel to the drift. This is a generalization of the continuity effect, a conclusion consistent with the previous simulation results (Ferguson 1986; Wang 1990). The coupling effect is embedded in the analysis by Reeks (1977).

The particle diffusivity and velocity scale based on the nonlinear drag were found to be larger than their equivalent values based on the Stokes drag. This result is consistent with the results of the numerical simulation (Wang and Stock 1992) and the analysis based on the Eulerian direct interaction (Reeks 1980). With the use of the effective inertia parameter and effective drift parameter, the increase in the particle diffusivity and velocity scale is shown to be due to the reduction of both the effective inertia and the effective drift when the nonlinear drag is used.

Unlike previous comprehensive analyses (Reeks 1977; Pismen and Nir 1978), the present analysis provides *algebraic* equations for long-time particle dispersion coefficients, time scales, and velocity scales. These algebraic equations can be used for parametric studies of engineering applications. For example, stochastic trajectory models (Walklate 1986, 1987) are very useful for simulating the dispersion of heavy particles in inhomogeneous flows (such as boundary-layer flows and jet flows), but they require relations for particle Lagrangian statistics. Use of the general results given in section 2c in a stochastic trajectory model will allow more precise and efficient simulation of heavy particle dispersion in complex flows.

We end this paper by mentioning two possible extensions of the analysis. First, the method of solving for the particle Lagrangian statistics can be applied to a decaying flow by incorporating the decay relations for the turbulence scales (Nir and Pismen 1979). Second, the analysis could be extended to the case of nonisotropic turbulence with a uniform shear (Riley and Corrsin 1974; Li and Meroney 1984). In this instance, the mean shear and the fluid Reynolds stress will both affect the dispersion.

Acknowledgments. This work was supported in part by funds of Summer Graduate Research Assistantship provided by Washington State University. Simulations were done on the University Computing Center's IBM 3090.

REFERENCES

Arnason, G., 1982: Measurement of particle dispersion in turbulent pipe flow. Ph.D. dissertation, Washington State University, Pullman, 183 pp.

——, and D. E. Stock, 1984: Dispersion of particles in turbulent pipe flow. *Gas Solid Flows,* **10,** 25–29.

Csanady, G. T., 1963: Turbulent diffusion of heavy particles in the atmosphere. *J. Atmos. Sci.,* **20,** 201–208.

——, 1973: *Turbulent Diffusion in the Environment.* D. Reidel, 248 pp.

Ferguson, J. R., 1986: The effects of fluid continuity on the turbulent dispersion of particles. Ph.D. dissertation, Washington State University, Pullman, 125 pp.

Friedlander, S. K., 1957: Behavior of suspended particles in a turbulent fluid. *AIChE J.,* **3**(3), 381–385.

Fung, J. C. H., J. C. R. Hunt, N. A. Malik, and R. J. Perkins, 1992: Kinematic simulation of homogeneous turbulence by unsteady random Fourier modes. *J. Fluid. Mech.,* **236,** 281–318.

Gouesbet, G., A. Berlemont, and A. Picart, 1984: Dispersion of discrete particles by continuous turbulent motion. Extensive discussion of the Tchen's theory, using a two-parameter family of Lagrangian correlation functions. *Phys. Fluids,* **27,** 827–837.

Hinze, J. O., 1975: *Turbulence.* McGraw-Hill, **253,** 460–471.

Kraichnan, R. H., 1964: Relation between Lagrangian and Eulerian correlation times of a turbulent velocity field. *Phys. Fluids,* **7,** 142–143.

Li, W. W., and R. N. Meroney, 1984: The estimation of atmospheric dispersion at nuclear power plants utilizing real time anemometer statistics. NRC-04-81-202, Colorado State University, Fort Collins, CO.

Lumley, J. L., 1957: Some problems connected with the motion of small particles in turbulent fluid. Ph.D. dissertation, The Johns Hopkins University, Baltimore, MD, 120 pp.

——, J. L., 1962: An approach to the Eulerian–Lagrangian problem. *J. Math. Phys.,* **3**(2), 309–312.

Lundgren, T. S., and Y. B. Pointin, 1976: Turbulent self-diffusion. *Phys. Fluids,* **19,** 1702–1711.

Maxey, M. R., 1987: The gravitational settling of aerosol particles in homogeneous turbulence and random flow fields. *J. Fluid Mech.,* **174,** 441–465.

——, and J. J. Riley, 1983: The equation of motion for small rigid particle sphere in a nonuniform flow. *Phys. Fluids,* **26,** 883–889.

Meek, C. C., and B. G. Jones, 1973: Studies of the behavior of heavy particles in a turbulent fluid flow. *J. Atmos. Sci.,* **30,** 239–244.

Mei, R., and R. J. Adrian, 1991: Particle dispersion in isotropic turbulence under Stokes drag and Basset force with gravitational settling. *J. Fluid Mech.,* **225,** 481–495.

Nichols, R. H., 1990: The effect of particle dynamics on turbulence measurements with the laser velocimeter. *Numerical Methods for Multiphase Flows,* I. Celik, D. Hughes, C. T. Crowe, and D. Lankford, Eds., FED-Vol. **91,** 35–45.

Nir, A., and L. M. Pismen, 1979: The effect of a steady drift on the dispersion of a particle in turbulent fluid. *J. Fluid Mech.,* **94,** 369–381.

Pasquill, P., and F. B. Smith, 1983: *Atmospheric Diffusion,* third ed. Ellis Harwood, 80–87.

Picart, A., A. Berlemont, and G. Gousbet, 1986: Modelling and predicting turbulent fields and the dispersion of discrete particles transported by turbulent flows. *Int. J. Multiphase Flow,* **12**(2), 237–261.

Pismen, L. M., and A. Nir, 1978: On the motion of suspended particles in stationary homogeneous turbulence. *J. Fluid Mech.,* **84,** 193–206.

Reeks, M. W., 1977: On the dispersion of small particles suspended in an isotropic turbulent field. *J. Fluid Mech.,* **83,** 529–546.

——, 1980: Eulerian direct interaction applied to the statistical motion of particles in a turbulent fluid. *J. Fluid Mech.,* **97,** 569–590.

Riley, J. J., and S. Corrsin, 1974: The relation of turbulent diffusivities to Lagrangian velocity statistics for the simplest shear flow. *J. Geophys. Res.,* **79,** 1768–1771.

Rowe, P. N., 1961: The drag coefficient of a sphere. *Trans. Inst. Chem. Eng.,* **39,** 175–181.

Sato, Y., and K. Yamamoto, 1987: Lagrangian measurement of fluid-

particle motion in an isotropic turbulent field. *J. Fluid Mech.*, **175,** 183–199.

Shlien, D. J., and S. Corrsin, 1974: A measurement of Lagrangian velocity correlation in approximately isotropic turbulence. *J. Fluid Mech.*, **62,** 255–271.

Snyder, W. H., and J. L. Lumley, 1971: Some measurements of particle velocity autocorrelation functions in a turbulent flow. *J. Fluid Mech.*, **48,** 41–71.

Soo, S. L., 1956: Statistical properties of momentum transfer in two-phase flow. *Chem. Eng. Sci.*, **5,** 57–67.

Taylor, G. I., 1921: Diffusion by continuous movements. *Proc. Roy. Soc. Ser. A,* **151,** 421–478.

Tchen, C. M., 1947: Mean value and correlation problems connected with the motion of small particles suspended in a turbulent fluid. Ph.D. dissertation, University of Delft, Martinus Nujhoff, The Hague, 125 pp.

Tennekes, H., 1979: The exponential Lagrangian correlation function and turbulent diffusion in the inertial subrange. *Atmos. Environ.*, **13,** 1565–1567.

Walklate, P. J., 1986: A Markov-chain particle dispersion model based on air flow data: extension to large water droplets. *Bound.-Layer Meteor.*, **37,** 313–318.

——, 1987: A random-walk model for dispersion of heavy particles in turbulent air flow. *Bound.-Layer Meteor.*, **39,** 175–190.

——, 1988: Reply to comments on a relationship between fluid and immersed-particle velocity fluctuations. *Bound.-Layer Meteor.*, **43,** 99–100.

Wang, L. P., 1990: On the dispersion of heavy particles by turbulent motion. Ph.D. dissertation, Washington State University, Pullman, WA,

——, and D. E. Stock, 1988: Theoretical method for obtaining Lagrangian statistics from measurable Eulerian statistics for homogeneous turbulence. *Proc. 11th Symp. on Turbulence,* Rolla, MS, B14.1–B14.12.

——, and ——, 1992: Numerical simulation of heavy particle dispersion: time step and nonlinear drag considerations. *J. Fluids Engr.*, **114,** 100–106.

Weinstock, J., 1976: Lagrangian–Eulerian relation and the independence approximation. *Phys. Fluids,* **19,** 1702–1711.

Wells, M. R., and D. E. Stock, 1983: The effects of crossing trajectories on the dispersion of particles in a turbulent flow. *J. Fluid Mech.*, **136,** 31–62.

Yeung, P. K., 1989: A study of Lagrangian statistics in stationary isotropic turbulence using direct numerical simulations, Ph.D. dissertation, Cornell University, Ithaca, NY, 217 pp.

Yudine, M. I., 1959: Physical considerations on heavy-particle dispersion. *Advances in Geophysics,* Vol. 6, Academic Press, 185–191.